

PAPER • OPEN ACCESS

High gravity-assisted green synthesis of ZnO nanoparticles via *Allium ursinum*: Conjoining nanochemistry to neuroscience

To cite this article: Navid Rabiee *et al* 2020 *Nano Ex.* 1 020025

View the [article online](#) for updates and enhancements.

Recent citations

- [Polymer-Coated NH₂-UiO-66 for the Codelivery of DOX/pCRISPR](#)
Navid Rabiee *et al*
- [Zn-rich \(GaN\)_{1-x}\(ZnO\)_x: a biomedical friend?](#)
Mojtaba Bagherzadeh *et al*
- [Nanotechnology-assisted microfluidic systems: from bench to bedside](#)
Navid Rabiee *et al*



ECS **240th ECS Meeting**
Digital Meeting, Oct 10-14, 2021

Register early and save up to 20% on registration costs

Early registration deadline Sep 13

REGISTER NOW



PAPER

OPEN ACCESS

RECEIVED
8 July 2020REVISED
28 July 2020ACCEPTED FOR PUBLICATION
4 August 2020PUBLISHED
14 August 2020

Original content from this work may be used under the terms of the [Creative Commons Attribution 4.0 licence](#).

Any further distribution of this work must maintain attribution to the author(s) and the title of the work, journal citation and DOI.



High gravity-assisted green synthesis of ZnO nanoparticles via *Allium ursinum*: Conjoining nanochemistry to neuroscience

Navid Rabiee¹ , Mojtaba Bagherzadeh^{1,5}, Mahsa Kiani¹, Amir Mohammad Ghadiri¹ , Kaiqiang Zhang², Zhong Jin², Seeram Ramakrishna³ and Mohammadreza Shokouhimehr^{4,5}

¹ Department of Chemistry, Sharif University of Technology, Tehran, Iran

² Jiangsu Key Laboratory of Advanced Organic Materials, Key Laboratory of Mesoscopic Chemistry of MOE, School of Chemistry and Chemical Engineering, Nanjing University, Nanjing, Jiangsu 210023, People's Republic of China

³ Center for Nanofibers and Nanotechnology, National University of Singapore, Singapore

⁴ Department of Materials Science and Engineering, Seoul National University, Seoul 08826, Republic of Korea

⁵ Authors to whom any correspondence should be addressed.

E-mail: bagherzadeh@sharif.edu and mrrsh2@snu.ac.kr

Keywords: zinc oxide, *Allium ursinum*, ZnO nanoparticles, antibacterial, green synthesis

Supplementary material for this article is available [online](#)

Abstract

This study aims to investigate the synthesis of ZnO nanoparticles (NPs) using high-gravity technique and mediated by novel *Allium ursinum* leaves' extract, which is derived for the first time. The synthesized NPs were fully characterized, and the potential biological activities were evaluated in the context of neuroscience. The size of the nanoparticles was found in range of 20 to 60 nm's, with a considerable size distribution of 30 nm; and their morphology are semi-spherical. More specifically the potential antibacterial activity against gram positive (*S. aureus*) and gram negative (*E. coli*) bacteria were screened. To the best of our knowledge, this study could be considered as the first investigation in the world, and the first comprehensive study on synthesizing ZnO NPs using high-gravity technique mediated by this plant extract. The experimental results were found to be very promising to the nanochemistry, green chemistry and also the applied neuroscience. In addition, the mentioned green synthesis procedure leads to the formation of NPs with considerable antibacterial, cellular proliferation and mitochondrial membrane potential as well as minimum apoptosis index and acceptable relative cell viability that are all independent with the morphology and texture of the media of these NPs. The green synthesized nanoparticles showed considerable antioxidant activity in comparison with the standard drug, more than 80%, and low cytotoxicity, more than 60% cellular viability in most of the concentrations, as well as proliferation inhibition of up to 84% in the maximum concentration. Along with those results, the mitochondrial membrane potential showed also promising absorption of over 1.6. Furthermore, the antioxidant activity of the green synthesized ZnO NPs was recorded above 82% which is greater than the standard BHT as well as the leaf extract

Introduction

In recent years, the use of different nanomaterials and nanoparticles in various industries such as water treatment, biomedical engineering, industrial and textile catalysts have flourished. The use of metal nanoparticles in various industries is of great importance, and the use of this type of nanomaterial is increasing every year [1, 2]. To this end, reducing the cost of preparing these nanomaterials, along with providing highly effective synthetic solutions, is the focus of scientists around the world. Different synthesis methods can lead to different yields as well as increasing/reducing the cost of the preparations [3, 4]. A variety of synthetic methods have been studied in recent decades, but in the last decade green synthesis methods have been considered. This method is nature-friendly, low-cost, leads to high-efficiency synthesis, and also does not cause specific toxicity to natural elements. In addition, in biological studies, as well as the biological applications of metal nanoparticles,

attention should be paid to the cellular toxicity that these nanoparticles can cause. Green synthesis methods use solvents such as water that do not cause cell toxicity, as well as stabilizers and reducing agents such as plants that are biodegradable and biodegradable [5, 6]. Above all of the mentioned advantageous of using green synthesis methods, the necessary of increasing the yield of nanoparticles synthesis, along with reducing the preparation costs as well as improving the stability of the synthesized NPs in different environments/ matrix lead the scientists to use green methodology for their synthesis procedures [7–10].

In recent years, scientists have been focused on using nanotechnology, nanochemistry and nanomedicine in early diagnosis, prevention and treatment of several diseases. In a meantime, with the invention of different range of nano devices, especially based on metal NPs, gene sequencing has attracted more attention [11, 12]. These metallic NPs have considerable effect on the electromagnetic, catalytic and biological properties. Currently, gold, iron, zinc, cobalt and silver NPs have been used widely in early diagnosis and treatment of different diseases based on pathogens, viral and parasites as well as in the treatment of refractory diseases such as cancer. Zinc NPs have been shown different features and applications from antibacterial and antifungal, towards gene therapy and neuroprotective effects [13, 14]. Recently, it has been revealed that zinc NPs could be able to decrease the neural inflammation as well as affecting on apoptosis and enhancing the neural antioxidant responses. In addition, it can be able to increase the infiltrating the immune cell, which makes it a good candidate for neuroprotective effect against different range of neurotoxins. In addition, the use of some physical techniques such as high-gravity has been considered widely to increase the potential of fast electron transfer in synthesis methods as well as enhancing the effective collision between different particles [15–20].

In this work, for the first time, we aim on green synthesis of zinc oxide NPs using high-gravity technique from *Allium ursinum* and studying the possible biomedical applications including catalytic, cellular viability, antioxidant activity, antibacterial activity, cellular proliferation and mitochondrial membrane potential investigations of these NPs. In addition, the role of green synthesis method and its relationship with the mentioned potentials was investigated.

Materials and methods

Chemicals, reagents and plant source

Allium ursinum leaves were collected from Shemiranat, Iran. *Staphylococcus aureus* (ATCC 25923TM) and *Escherichia coli* (ATCC 25922TM) spores were used. All of the chemicals and reagents were of analytical grade and obtained from Sigma-Aldrich, Germany.

Preparation of plant extract

For the preparation of the plant extract, the collected *Allium ursinum* was washed for three times with ethanol and deionized water, and dried at room temperature. The dried plant was transferred to a mortar and turns to a fine powder. In the next step, the powders were placed on a heater stirrer and dispersed in the deionized water (stirring for 35 min at 70 °C). The obtained suspension was filtered carefully and stored at 4 °C for further procedures.

ZnO NPs synthesis procedure

To achieve these NPs from the *Allium ursinum* leaf broth, rotating packed bed (RPB) system with some modifications was applied. 40 ml of *Allium ursinum* was poured into 160 ml of the zinc nitrate solution (1 mM) and the suspension was stirred for 15 min at 75 °C. After that, the final suspension was transferred to the RPB system and the mixing of the precipitation process was conducted inside the internal circulation of the RPB system. The synthesized NPs were filtered and centrifuged at 12,000 rpm for about 20 min. It should be noted that, there is several protocols for controlling and adjusting the gravity in this technique and modified one, and in this study, high gravity levels were provided by adjusting the speed of rotation in the RPB with the 1400 rpm. Also, the exact value of the outer radius packing system is 100 cm and the inner one if about 34 cm. The synthesized NPs were filtered and centrifuged at 12,000 rpm for about 20 min. Furthermore, by the equation of Wu *et al* research group [21, 22], the corresponding mean high gravity level (β) is calculated 182 in this study.

$$\beta = \frac{\int_{r_1}^{r_2} 2\pi r \beta dr}{\int_{r_1}^{r_2} 2\pi r dr} = \frac{2\omega^2(r_1^2 + r_1 r_2 + r_2^2)}{3(r_1 + r_2)g}$$

In the above equation, inner radius and outer radius of packing are assigned by r_1 and r_2 , and ω corresponds to the rotor speed (rad s^{-1}), and also the value of the gravity acceleration (g) considered to be 9.8 m s^{-2} .

Characterization of synthesized NPs

The characterization techniques were applied same as our previous publications [7–9]. UV–vis spectrometer (Perkin Elmer Lambda 25) was applied to record absorbance of ZnO NPs in the range of 200–800 nm. Fourier transformed infrared spectroscopy (FT-IR) spectrum was applied using JASCO FT-IR-460 spectrometer in the range of 400–4000 cm^{-1} . Powdered x-ray diffraction (PXRD) spectra were obtained by an automated Philips X'Pert x-ray diffractometer with Cu K α radiation (40 kV and 30 mA) for 2θ values over the range of 10–80. The morphology of synthesized ZnO NPs was observed by field emission scanning electron microscope (FESEM, TESCAN MIRA-3) under an acceleration voltage of 30–250 kV.

Antibacterial activity

The antibacterial activity of the green synthesized nanoparticles in assistance of high-gravity was investigated based on the literature [23–25].

The green synthesized nanoparticles and the leaf extracts were applied for the culture on the agar plate for *Staphylococcus aureus* and *Escherichia coli* bacteria's. One plate with two section for the NPs (1) and the extract (2), another plate with four section for the water (negative control), DMSO (Solvent) and the standard (Penicillin and Gentamycin, positive control) were used. After that, 15 μl of the samples (sterile samples) was injected on the paper disc and dried at room temperature. The obtained plates were incubated at 37 °C for 24 h and the antibacterial activities were calculated as diameter zone of inhibitive.

Antioxidant activity

For this purpose, radical scavenging of 2,2-diphenyl-1-picrylhydrazyl (DPPH) was evaluated by the methanol solution of DPPH discoloration, to be exact, the discoloration process is performed by the mechanism based on the reduction of DPPH. In this manner, the DPPH solution reacts with the reducing agent (the synthesized nanoparticle and the plant extract) and the color of the DPPH changes from violet to yellow. Different concentrations of BHT, the leaf extract as well as the green synthesized ZnO NPs from 0 to 1000 $\mu\text{g ml}^{-1}$ were used in a period of time of 12 h treatment, and the temperature of this experiment was maintained at 37 °C. To investigate the exact color change and intensity, a microplate reader was applied at 517 nm, and the solution were measured at this wavelength after about 30 min of vigorous stirring. The positive control is butylated hydroxytoluene (BHT) and the radical scavenging of DPPH activity was investigated as the percentage of inhibition, calculated as follows:

DPPH radical scavenging activity (%) = [(control absorbance—sample absorbance)/control absorbance] \times 100. This analysis was performed three times, and the curves of inhibition were drawn based on the sample concentration that requires to scavenging the half of the DPPH free radical, IC50.

Cell culture

The PC12 (ATCC CRL-1721TM) cells were used in the following assays. PC12 cells were grown in DMEM (Gibco, Invitrogen, Norway) (supplemented with 1 mM amino acids (non-essential one's) and fetal bovine serum (10%), (FBS) and 5% CO₂ at 37 °C). Since methadone will change the cellular morphology, the apoptotic cells would result in cellular treatment by 100 μM of the drug. In this case, the treatment with the nanoparticles and the leaf extracts was performed for 12 h, and after that, the cells were washed by PBS and classified as follows: (a) the drug, methadone; (b) culture medium without any drug as the control group; (c) cell culture including the drug (100 μM of methadone) and 1 μg of the leaf extract; (d) cell culture including the drug (100 μM of methadone) and the leaf extract (2 μg); (e) cell culture including the drug (100 μM of methadone) and the leaf extract (5 μg); (f) cell culture including the drug (100 μM of methadone) and the synthesized nanoparticle (1 μg); (g) cell culture including the drug (100 μM of methadone) and the synthesized nanoparticle (2 μg); (h) cell culture including the drug (100 μM of methadone) and the synthesized nanoparticle (5 μg).

MTT assay

The cytotoxicity, cellular proliferation and all of the related assays were performed on the PC12 cell line based on the protocols in the literature [26–28]. The PC12 cells were seeded (on a 96 well-plate substrate) with the density of 2×10^5 cells/well. The seeded cells were incubated for 24 h with 100 μl of DMEM/F12 and 10% FBS. In the next step, the culture media was replaced with the exact dilutions of the sterilized samples and incubated for more 6 h. The obtained well-plates media were replaced with 100 μl of the culture media that have been included MTT and incubated for more 5 h at 37 °C. The resulted medium was aspirated and the MTT formazan dissolved in DMSO (100 μl). Finally, the absorbance spectra of the resulted well-plates was screened by using a microplate reader (570 nm).

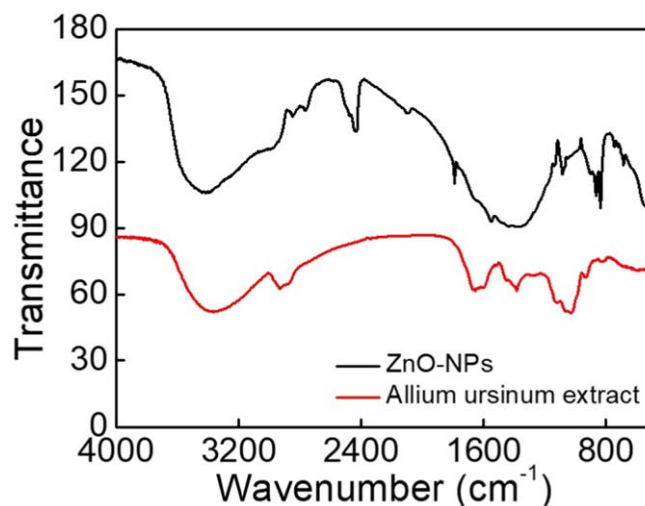


Figure 1. FTIR spectra of *Allium ursinum* extract and the green synthesized ZnO NPs in assistance of high-gravity.

The potential of mitochondrial membrane

In this step, the treatments were exposed to an exact concentration of rhodamine-123 for 30 min, and the cellular matrix were washed for several times by PBS. In the following, triton X-100 (900 μl) was added dropwise to each well (kept for 2 h in 4 °C). The resulted solutions were centrifuged at 14,000 rpm for 30 min, and the microplate reader (excitation wavelength at 488 nm and the emission wavelength at 520 nm) was applied for the measurements.

Statistical analysis

For all of the assays, one-way analysis of variance (ANOVA) followed by OriginPro 9.1 software was applied and all of the obtained data's was generated via $\pm\text{SD}$ of at least $n = 3$ independent sets of experiments.

Results and discussion

FTIR results

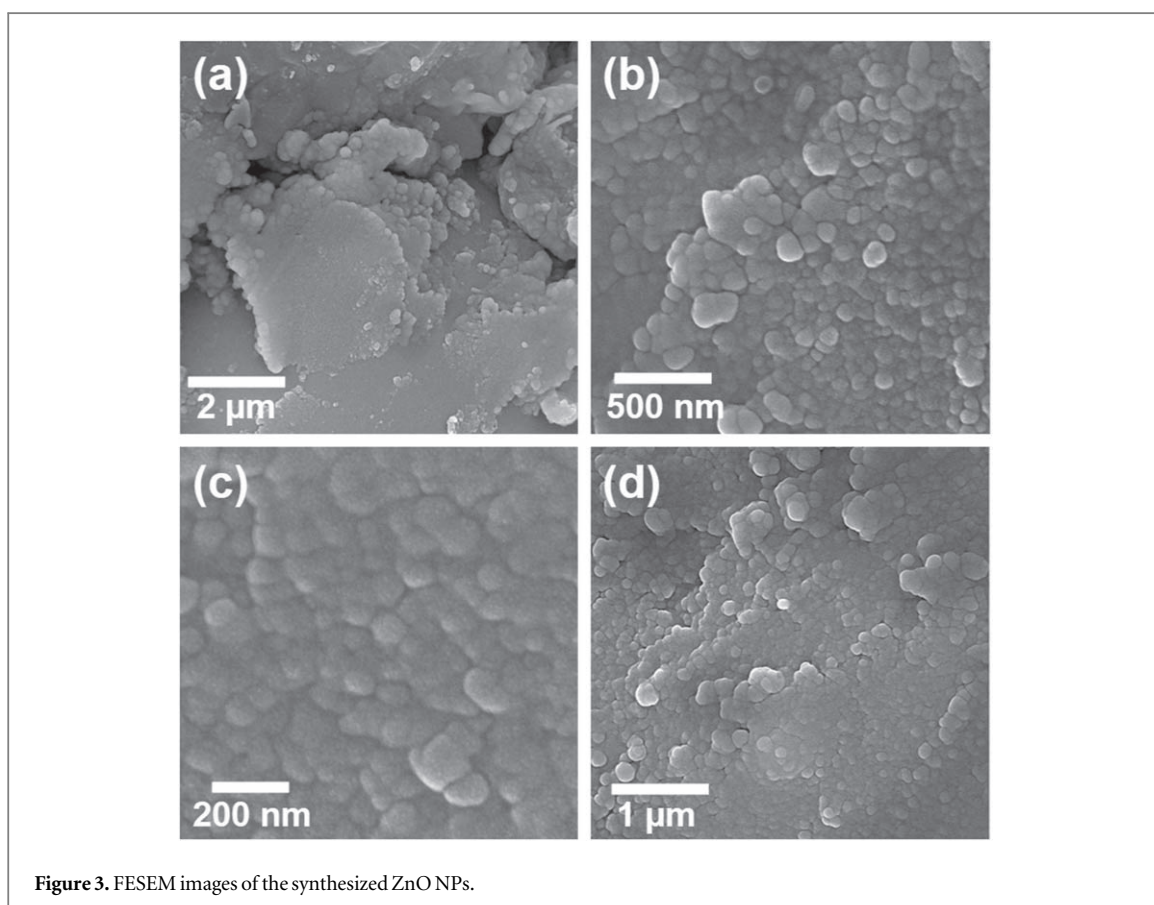
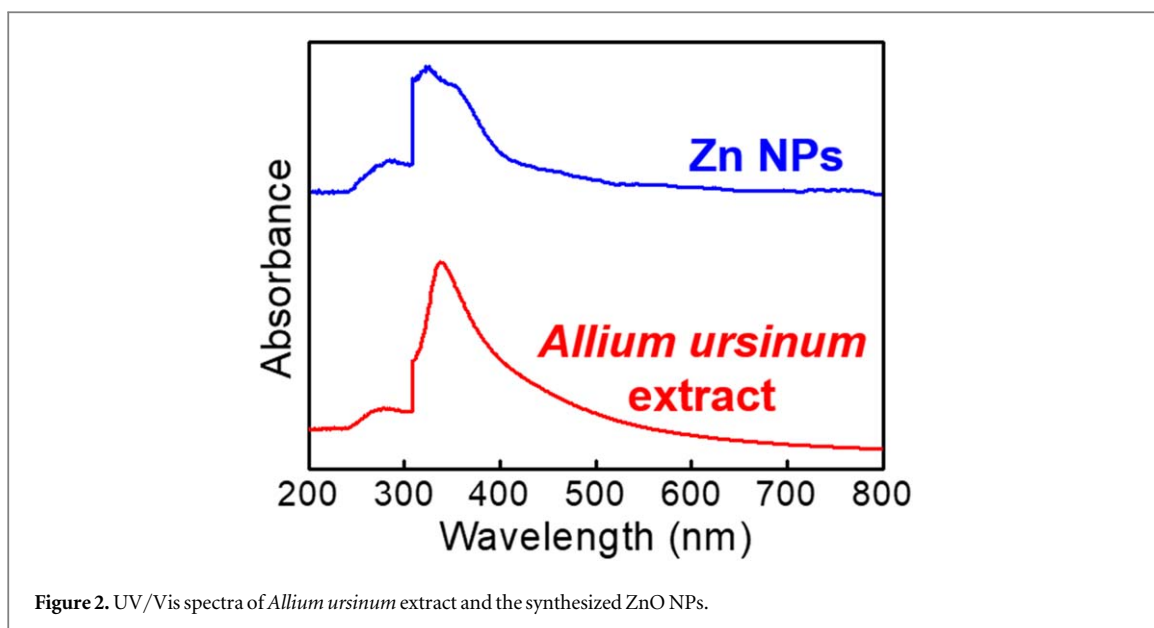
FTIR spectra of the green synthesized zinc oxide NPs in assistance of high-gravity mediated by *Allium ursinum* shown in figure 1. The band at 3400 cm^{-1} corresponds to the stretching frequency of O–H groups. The peak at 1050 cm^{-1} represents the ester bonds between the nanoparticles and polar O–H groups. Furthermore, a shoulder like peak at around 540 cm^{-1} indicates the ZnO absorption band, which is clearly overlap with the band of the chemical composition of the leaf extract. Also, a series of peaks around 1500 cm^{-1} , 1330 cm^{-1} and 940 cm^{-1} are assigned to the presence of –OH stretching bond due to the intramolecular hydrogen bonding and stretching band of C=O and also C–C of alkanes [29–31]. The FTIR of *Allium ursinum* clearly showed, after purification and leaf extraction, most of the chemical composition of the garlic-based materials remains, but some peaks around 1200 cm^{-1} and 1550 cm^{-1} disappeared or weakened, however, the main neuroprotective chemical composition of garlic in *Allium ursinum* that comes from derivatives of cysteine are remained.

UV–vis spectra analysis

The UV–vis spectra of the synthesized nanoparticles and the leaf extract was shown in figure 2, indicates an absorbance at 335 nm to 355 nm that is an index of ZnO phases [23, 32]. Another absorbance in the range of 310 to 330 nm corresponds to the presence of the extract leaf, which is in strong overlap with ZnO peak and make a wide peak from 310 to 360 nm [33–35]. The wide size distribution of the nanoparticles that is because of the green and high-gravity method, leads to the broadness of the absorption peak.

Morphology analysis

The FESEM technique was applied to investigate the surface morphology of the synthesized nanoparticles (figure 3). Zinc oxide NPs by this method show nearly monodispersed distribution of particle sizes. The average particle size of the ZnO NPs is smaller than 30 nm (however, there are nanoparticles in the range of 30 to 60 nm's as well). Based on the results, by ignoring the aggregations, the nanoparticles shape and morphology can be considered to be semi-spherical. By using a green method in synthesis of the nanoparticles, more aggregations



were expected due to the presence of leaf extract and the remaining plant compartments, however, by applying the high-gravity technique, those aggregations were directed to the synthesis with high yield [36–38].

XRD analysis

XRD analysis was conducted to prove the structural chemistry of the green synthesized ZnO NPs (figure 4). The main characteristic diffraction peaks for ZnO NPs are at around $2\theta = 31^\circ, 34^\circ, 36^\circ, 47^\circ, 56^\circ, 63^\circ, 67^\circ$ and 69° which correspond to the (100), (002), (101), (102), (110), (103), (112) and (201) crystallographic planes of wurtzite ZnO (JCPDS card No. 36–1451), respectively [39–41].

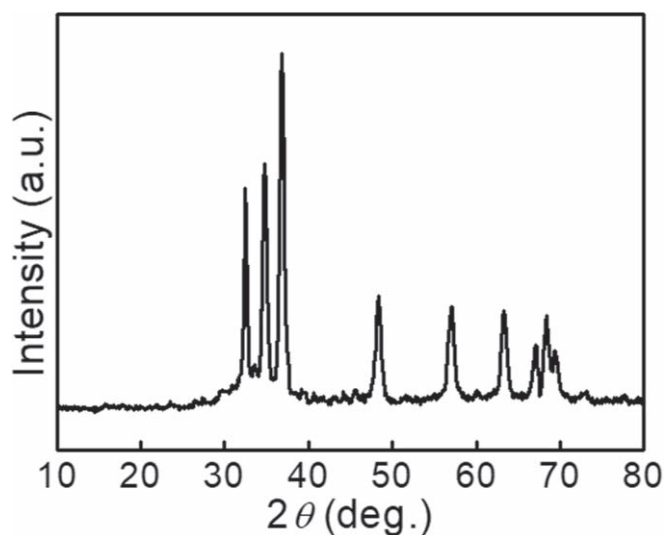


Figure 4. XRD pattern of the synthesized ZnO NPs.

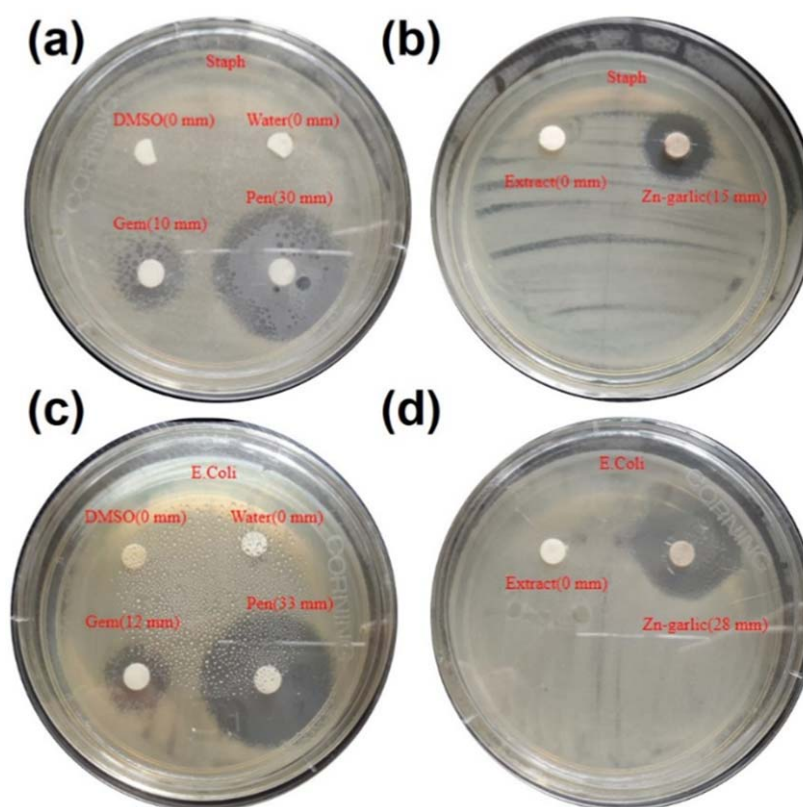


Figure 5. Antibacterial effect of the controls and green synthesized nanoparticles on *Staph* (a) and (b), and on *E. coli* (c) and (d).

Antibacterial activity

In this step, the potential antibacterial activity of the synthesized NPs, ZnO NPs, were screened against *S. aureus* as the gram positive bacteria and *E. coli* and the gram negative one by the well-known method, agar disc diffusion technique (figure 5). The different bacterial strains of zone inhibition are shown in figure 6. The ZnO NPs shows higher antibacterial activity against *E. coli* these NPs show higher MZI against compared to the standard at 25 mg ml^{-1} . These NPs break of the cell wall, causing membrane damage. This leads to killing of bacteria. The green synthesis procedure the media and structure of NPs showing considerable antibacterial activities.

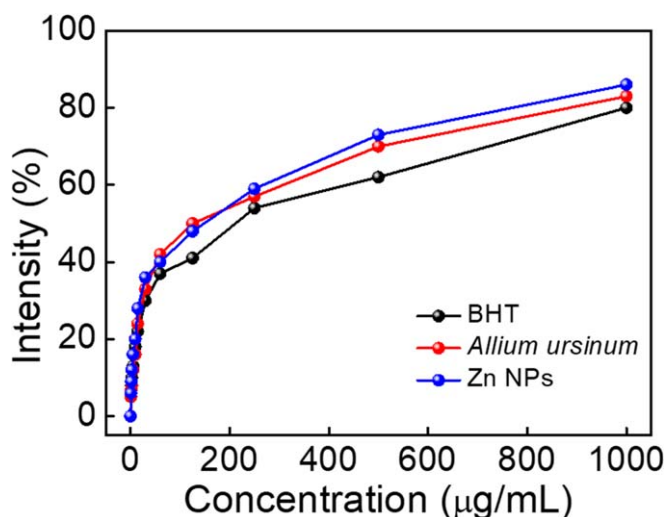


Figure 6. Antioxidant activity of *Allium ursinum* and the synthesized ZnO NPs in comparison with BHT.

Antioxidant activity

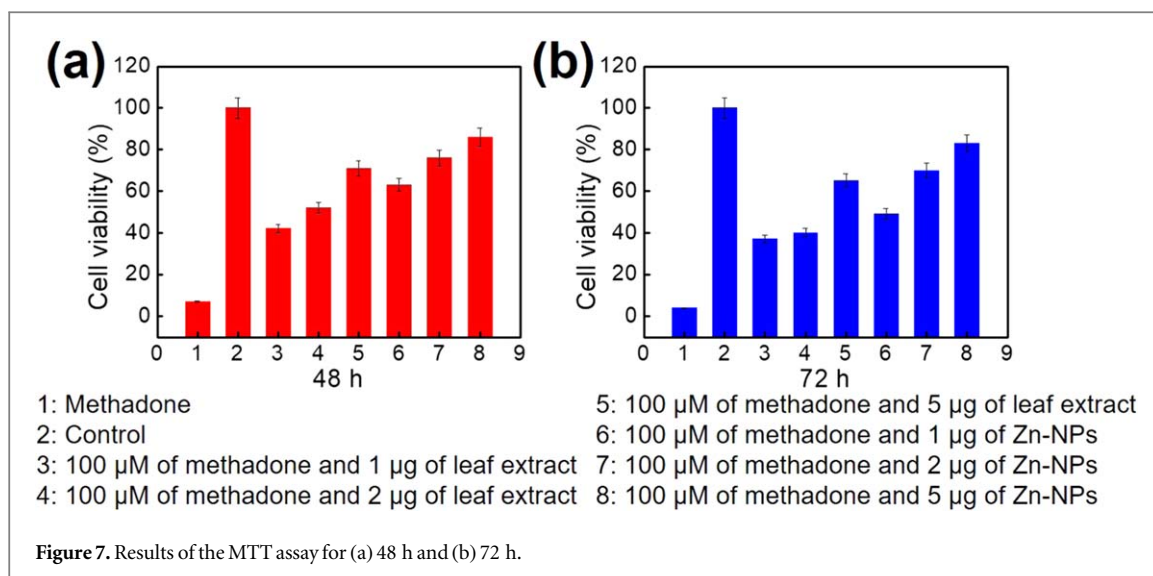
In the last decade, several research groups focused on synthesizing the new or modifying the natural compounds to act as antioxidant additives [42–44]. In this manner, using a simple and eco-friendly synthesizing methods that have been leads to obtain a product with promising antioxidant activity would have great importance [45–47]. The extract leaves of some plants such as *Allium saralicum* [48], *Allium sativum* [49] and *Falcaria vulgaris* [50] were shown an acceptable antioxidant activity, which is resulted of the free radicals degradations. In this process, by reduction of the concentration levels of glutathione (GSH), the serum concentrations levels of glutathione peroxidase (GPx), malodialdehyde (MDA), plasma catalase (CAT) and superoxide dismutase (SOD) will increase considerably [51–54]. In addition, based on the GC-Mass results of the *Allium ursinum* (supporting information is available online at stacks.iop.org/NANOX/1/020025/mmedia), the *Allium ursinum* contains several complex structure including flavonoids, alkaloids and also phenolic compounds which all have significant antioxidant effects in the biological systems, which is same as the garlic and *Allium sativum* structure [55–57]. A professional approach to increase the antioxidant property could be to synthesize the NPs via a green rout with this class of plants. Various NPs have been reported, but one of the best one in terms of biological properties can be zinc. In this study, we have been investigated the antioxidant potential of ZnO NPs and *Allium ursinum* in comparison with BHT in terms of their suppressor capacity on cell death of methadone-induced culture in PC12 cell line.

The *in vitro* analysis of radical inhibitory of DPPH was performed based on the ability of antioxidant hydrogen donating to DPPH radical reduce to form the non-radical DPPH-H. Based on the results, a similar trends that comes from concentration dependency of the nanomaterials shown for ZnO NPs and *Allium ursinum* in comparison with BHT, which would be because of strong electron transfer that leads to form a stable DPPH molecule. Both ZnO NPs and *Allium ursinum* shows higher antioxidant activity than BHT. For *Allium ursinum*, the antioxidant activity is because of the presence of flavonoids, alkaloids and also phenolic compounds (based on the GC-Mass) (Supporting informaiton), which can be able to absorbed free radicals and neutralize the radical forms, and for ZnO NPs, both the natural structure of the synthesizing media and the electronic effect of d-orbitals have significant effect on this results.

Based on the literature [58–60], these results (figure 6) that have been adopted from a simple, cost-effective, green and one-pot synthesizing method considered as a promising rout for achieving a metallic nanoparticle with several potentials.

Cytotoxicity and cellular proliferation

Methadone and other opioid dependence drugs are used to treat, and also prevent, acute and chronic pains, and in some cases opioid addiction treatments, however, long-term using of this types of drugs would certainly leads to serious neurotoxic effects [61–63]. The mechanism of these types of drugs in the body directly effects the central nervous system, via changing the morphology and in some cases the length of the receptors which leads to serious problems in mid- and long-terms consumption of these drugs. In addition, these drugs, especially methadone, can have significant adverse effect on the brain, in the deep white matter of the cerebral hemispheres and also basal ganglia as well as cerebellum, which itself leads to personality disorders, psychosis, acute respiratory diseases and also death due to stroke. These are resulted from manipulation and destruction of two



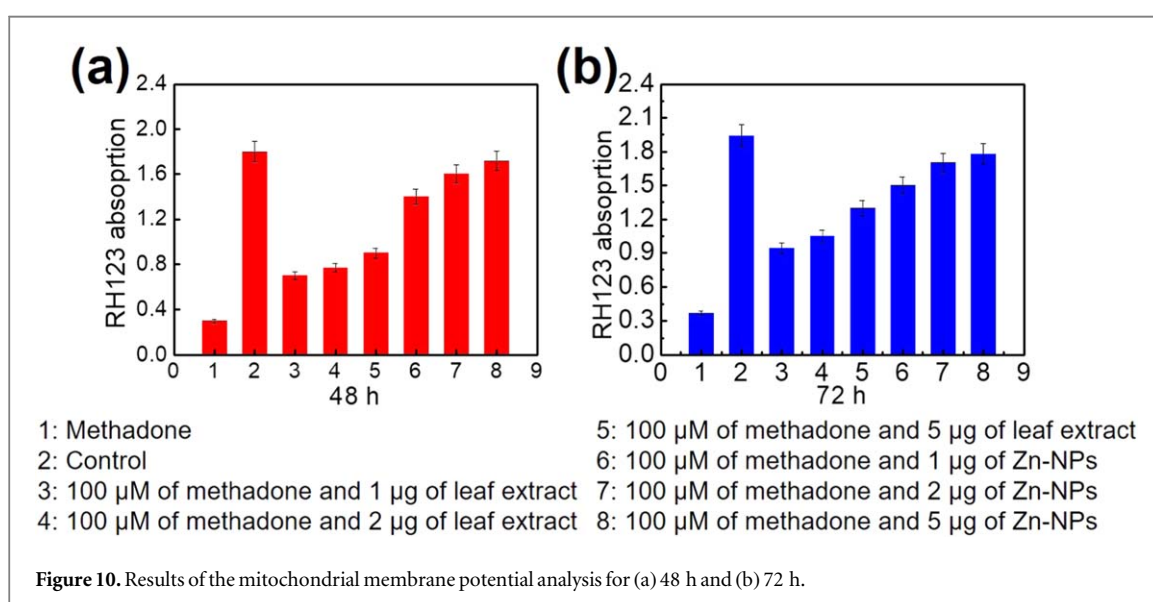
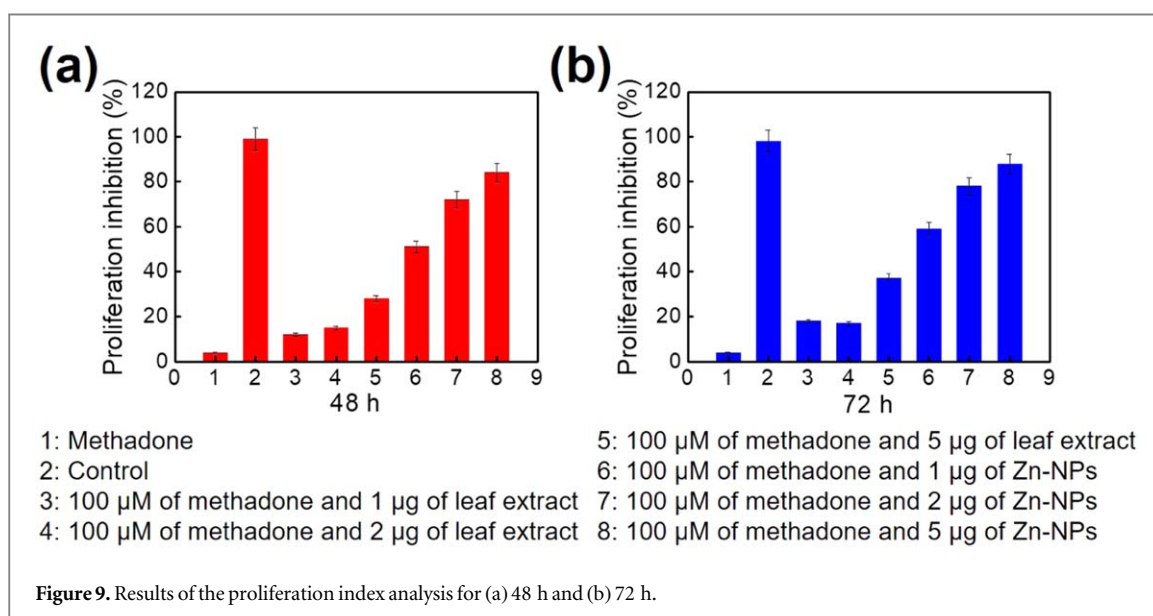
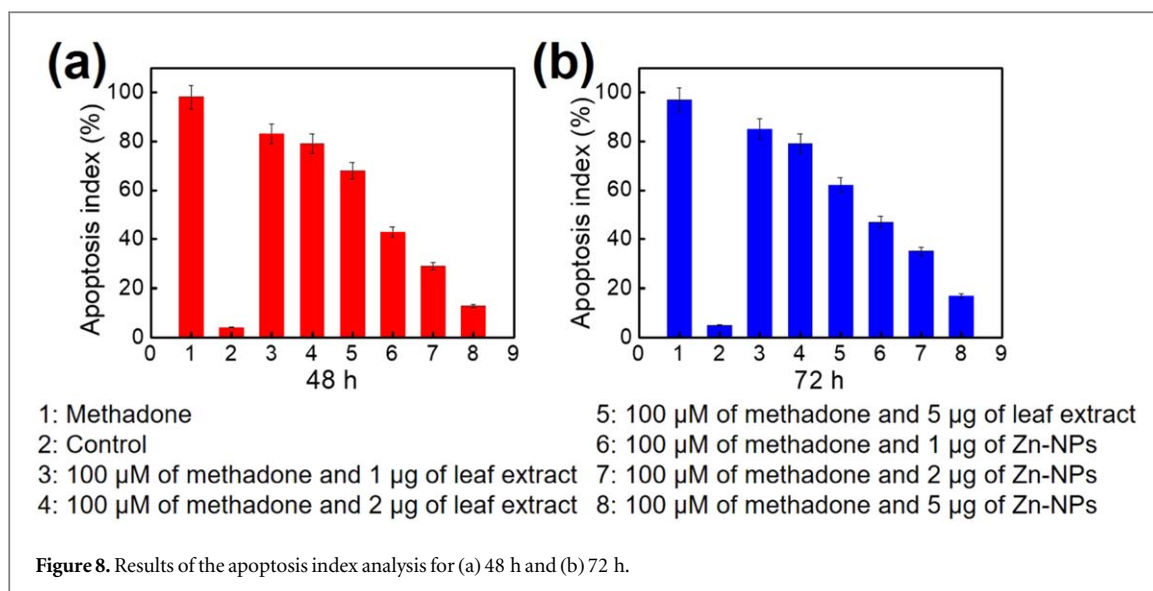
signal pathways that the methadone effects, antagonism in NMDR and bindings to opioid receptors, which the first one is more critical and important. Furthermore, treatment with methadone for a long-term would cause a considerable increase in the levels of interleukin 1 beta as well as interleukin 6 and tumor necrosis factor alpha [64–67].

The results of our study (figure 7) indicate that high dose of opioids drugs, especially methadone, causes considerable reduction in cell viability which leads to cytotoxicity as well as increasing the potential of nerve cell lines, in this study PC12, which are in agreement with the literature [68–71]. However, by combining these cells with ZnO NPs and with the leaf extract, the cell viability increased substantially and the cellular toxicity decreases gradually which leads to enhancing the potential of cell proliferation. Certainly, reducing the cytotoxicity of neuron cells in the presence of ZnO NPs and the leaf extract is because of the antioxidant activity of these compounds, which comes from the mechanism of inhibition of reactive oxygens in these structures and cellular oxidative stresses.

From another perspective, these opioids drugs, especially methadone, can be able to activate the apoptosis pathway of mitochondria with a mechanism similar to the methadone activities. In this manner, b-cell lymphoma 2 is considered as the apoptosis mitochondrial regulator, which causes several changes in the mitochondria. To be exact, by producing free radicals, the morphology of the surface of these mitochondria's changes to formation of several pores in the membrane, and by formation of these pores, lots of compounds and factors can release significantly from the membrane to the cytoplasm including caspase 2 and 9, cytochrome C and also the factors related to inducing apoptosis. In this regard, increasing the chemical absorption of rhodamine 123 leads to improving the potential of the membrane of mitochondria's that is a proof of enhancing the activity of proton pumps. The results of this study (figures 8–10) revealed that these opioid drugs, especially methadone, can be able to fragment the DNA and increase the PC12 cells apoptosis process. In addition, this apoptosis process enhanced by significant decrease in the potential of mitochondrial membrane, and this study revealed that the green synthesized ZnO NPs can increase this apoptosis process as well as decreasing the potential of mitochondrial membrane.

Future research

The results of this study showed that by using the basic rules of physics and chemistry, different results can be obtained from the initial results. In the meantime, by using the high gravity technique, and with the related physical manipulations, more stable nanoparticles in a certain size range can be achieved, which is a great help for specific biological applications. Investigating the morphological changes of these nanoparticles and nanomaterials, and the potential relationship between the surface morphology and the potential biomedical applications, especially in neuroscience, would be considered as the goals of future research. It should be noted that so far the effect of high gravity on different syntheses has resulted in size and morphology, but there may have been differences in electronic levels as well as electronic arrangement, which in turn can lead to different physical and chemical properties.



Conclusions

This study aims to investigate, for the first time, the new green and eco-friendly synthesizing method based on the ZnO NPs assisted high gravity mediated with leaves extracts. Based on the results, the green synthesized nanoparticles showed considerable antioxidant activity in comparison with the standard drug, more than 80%, and low cytotoxicity, more than 60% cellular viability in most of the concentrations, as well as proliferation inhibition of up to 84% in the maximum concentration. Along with those results, the mitochondrial membrane potential showed also promising absorption of over 1.6. Furthermore, the antioxidant activity of the green synthesized ZnO NPs was recorded above 82% which is greater than the standard BHT as well as the leaf extract. This work is the first investigation of synthesizing ZnO NPs mediated by this plant extract, which is a comprehensive study in connection between the nano-chemistry, green chemistry and neuroscience. In addition, the mentioned green synthesis procedure leads to the formation of NPs with considerable cellular proliferation, mitochondrial membrane potential and minimum apoptosis as well as acceptable relative cell viability that are independent with the morphology and texture of the media of these NPs.

Acknowledgments

Support of this work by the Sharif University of Technology Research Council is gratefully acknowledged. Furthermore, the financial supports of the Future Material Discovery Program (2016M3D1A1027666), the Basic Science Research Program (2017R1A2B3009135) through the National Research Foundation of Korea, and China Scholarship Council (201808260042) are appreciated.

Declaration of interest statement

The authors declare that they have no conflicts of interests to this work.

ORCID iDs

Navid Rabiee  <https://orcid.org/0000-0002-6945-8541>

Amir Mohammad Ghadiri  <https://orcid.org/0000-0003-4393-5837>

Mohammadreza Shokouhimehr  <https://orcid.org/0000-0003-1416-6805>

References

- [1] Kiani M et al 2020 Catalytic and antibacterial properties of 3-dentate carboxamide Pd/Pt complexes obtained via a benign route. *Appl. Organomet. Chem.* **34** e5531
- [2] Parsa S F et al 2018 Early diagnosis of disease using microbead array technology: a review *Anal. Chim. Acta* **1032** 1–17
- [3] Darbasizadeh B et al 2019 Crosslinked-polyvinyl alcohol-carboxymethyl cellulose/ZnO nanocomposite fibrous mats containing erythromycin (PVA-CMC/ZnO-EM): fabrication, characterization and in-vitro release and anti-bacterial properties *Int. J. Biol. Macromol.* **141** 1137–46
- [4] Iravani S 2011 Green synthesis of metal nanoparticles using plants *Green Chem.* **13** 2638–50
- [5] Nour S et al 2019 Bioactive materials: a comprehensive review on interactions with biological microenvironment based on the immune response *J. Bionic Eng.* **16** 563–81
- [6] Nik A B et al 2020 Smart drug delivery: capping strategies for mesoporous silica nanoparticles *Microporous Mesoporous Mater.* **299** 110115
- [7] Ghadiri A M et al 2020 Green synthesis of CuO-and Cu₂O-NPs in assistance with high-gravity: the flowering of Nanobiotechnology *Nanotechnology* (<https://doi.org/10.1088/1361-6528/aba142>)
- [8] Rabiee N et al 2020 Rosmarinus officinalis directed palladium nanoparticle synthesis: investigation of potential anti-bacterial, anti-fungal and Mizoroki-Heck catalytic activities *Adv. Powder Technol.* **31** 1402-1411
- [9] Rabiee N et al 2020 Biosynthesis of copper oxide nanoparticles with potential biomedical applications *Int. J. Nanomed.* **15** 3983–99
- [10] Vafajoo A, Salarian R and Rabiee N 2018 Biofunctionalized microbead arrays for early diagnosis of breast cancer *Biomed. Phys. Eng. Express* **4** (6) 065028
- [11] Maghsoudi S et al 2019 Recent advancements in aptamer-bioconjugates: sharpening stones for breast and prostate cancers targeting *J. Drug Delivery Sci. Technol.* **53** 101146
- [12] Maghsoudi S et al 2020 Burgeoning polymer nano blends for improved controlled drug release: a review *Int. J. Nanomed.* **15** 4363
- [13] Bharathi D and Bhuvaneshwari V 2019 Synthesis of zinc oxide nanoparticles (ZnO NPs) using pure bioflavonoid rutin and their biomedical applications: antibacterial, antioxidant and cytotoxic activities *Res. Chem. Intermed.* **45** 2065–78
- [14] Bharathi D et al 2019 Preparation of chitosan coated zinc oxide nanocomposite for enhanced antibacterial and photocatalytic activity: as a bionanocomposite *Int. J. Biol. Macromol.* **129** 989–96
- [15] Xia T et al 2008 Comparison of the mechanism of toxicity of zinc oxide and cerium oxide nanoparticles based on dissolution and oxidative stress properties *ACS Nano* **2** 2121–34
- [16] Kim T and Hyeon T 2013 Applications of inorganic nanoparticles as therapeutic agents *Nanotechnology* **25** 012001

- [17] Yang Q *et al* 2017 Neuroprotective effects of the nanoparticles of zinc sapogenin from seeds of camellia oleifera *J. Nanosci. Nanotechnol.* **17** 2394–400
- [18] Chen L and Gao X 2017 The application of nanoparticles for neuroprotection in acute ischemic stroke *Therapeutic Delivery* **8** 915–28
- [19] Sobieszczanska M *et al* 2012 Is the zinc neuroprotective effect caused by prevention of intracellular zinc accumulation *Adv. Clin. Exp. Med.* **21** (2) 245–8
- [20] Levenson C W 2005 Zinc supplementation: neuroprotective or neurotoxic? *Nutrition Reviews* **63** (4) 122–5
- [21] Wu K *et al* 2016 A novel routine for the fabrication of Y-type oxotitanium phthalocyanine nanocrystals in high-gravity rotating packed beds *Ind. Eng. Chem. Res.* **55** 6753–9
- [22] Wu K *et al* 2018 Controlling nucleation and fabricating nanoparticulate formulation of sorafenib using a high-gravity rotating packed bed *Ind. Eng. Chem. Res.* **57** (6) 1903–11
- [23] Raja A *et al* 2018 Eco-friendly preparation of zinc oxide nanoparticles using *Tabernaemontana divaricata* and its photocatalytic and antimicrobial activity *J. Photochem. Photobiol. B* **181** 53–8
- [24] Karthik K *et al* 2018 Multifunctional properties of microwave assisted CdO–NiO–ZnO mixed metal oxide nanocomposite: enhanced photocatalytic and antibacterial activities *J. Mater. Sci., Mater. Electron.* **29** 5459–71
- [25] Samu G F *et al* 2017 Photocatalytic, photoelectrochemical, and antibacterial activity of benign-by-design mechanochemically synthesized metal oxide nanomaterials *Catal. Today* **284** 3–10
- [26] Rai Y *et al* 2018 Mitochondrial biogenesis and metabolic hyperactivation limits the application of MTT assay in the estimation of radiation induced growth inhibition *Sci. Rep.* **8** 1–15.
- [27] Miri A and Sarani M 2018 Biosynthesis, characterization and cytotoxic activity of CeO₂ nanoparticles *Ceram. Int.* **44** 12642–7
- [28] Hamishehkar H *et al* 2018 Preparation, characterization and anti-proliferative effects of sclereol-loaded solid lipid nanoparticles on A549 human lung epithelial cancer cells *J. Drug Delivery Sci. Technol.* **45** 272–80
- [29] Sangeetha G, Rajeshwari S and Venkatesh R 2011 Green synthesis of zinc oxide nanoparticles by aloe barbadensis miller leaf extract: structure and optical properties *Mater. Res. Bull.* **46** 2560–6
- [30] Salam H A, Sivaraj R and Venkatesh R 2014 Green synthesis and characterization of zinc oxide nanoparticles from *Ocimum basilicum* L. var. *purpurascens* Benth.-Lamiaceae leaf extract *Mater. Lett.* **131** 16–8
- [31] Bala N *et al* 2015 Green synthesis of zinc oxide nanoparticles using *Hibiscus subdariffa* leaf extract: effect of temperature on synthesis, anti-bacterial activity and anti-diabetic activity *RSC Adv.* **5** 4993–5003
- [32] Vijayakumar S *et al* 2018 Green synthesis of zinc oxide nanoparticles using *Atalantia monophylla* leaf extracts: characterization and antimicrobial analysis *Mater. Sci. Semicond. Process.* **82** 39–45
- [33] Fahimmunisha B A *et al* 2020 Green fabrication, characterization and antibacterial potential of zinc oxide nanoparticles using *Aloe socotrina* leaf extract: a novel drug delivery approach *J. Drug Delivery Sci. Technol.* **55** 101465
- [34] Bayrami A *et al* 2019 Enriched zinc oxide nanoparticles by *Nasturtium officinale* leaf extract: joint ultrasound-microwave-facilitated synthesis, characterization, and implementation for diabetes control and bacterial inhibition *Ultrason. Sonochem.* **58** 104613
- [35] Abbasi B A *et al* 2020 Bioactivities of geranium wallichianum leaf extracts conjugated with zinc oxide nanoparticles *Biomolecules* **10** 38
- [36] Nemati S *et al* 2019 Cytotoxicity and photocatalytic applications of biosynthesized ZnO nanoparticles by *Rheum turketicum* rhizome extract *Mater. Res. Express* **6** 125016
- [37] Miri A *et al* 2019 Zinc oxide nanoparticles: biosynthesis, characterization, antifungal and cytotoxic activity *Materials Science and Engineering: C* **104** 109981
- [38] Miri A and Sarani M 2019 Biosynthesis and cytotoxic study of synthesized zinc oxide nanoparticles using *Salvadora persica* *BioNanoScience* **9** 164–71
- [39] Sivaraj R *et al* 2014 Biogenic copper oxide nanoparticles synthesis using *Tabernaemontana divaricata* leaf extract and its antibacterial activity against urinary tract pathogen *Spectrochim. Acta, Part A* **133** 178–81
- [40] Sankar R *et al* 2014 Green synthesis of colloidal copper oxide nanoparticles using *Carica papaya* and its application in photocatalytic dye degradation *Spectrochim. Acta, Part A* **121** 746–50
- [41] Nagar N and Devra V 2018 Green synthesis and characterization of copper nanoparticles using *Azadirachta indica* leaves *Mater. Chem. Phys.* **213** 44–51
- [42] Scampicchio M *et al* 2006 Nanoparticle-based assays of antioxidant activity *Anal. Chem.* **78** 2060–3
- [43] Das D *et al* 2013 Synthesis and evaluation of antioxidant and antibacterial behavior of CuO nanoparticles *Colloids Surf. B* **101** 430–3
- [44] Shibuya S *et al* 2014 Palladium and platinum nanoparticles attenuate aging-like skin atrophy via antioxidant activity in mice *PLoS One* **9** e109288
- [45] Ravichandran V *et al* 2016 Green synthesis of silver nanoparticles using *Atrocarpus altilis* leaf extract and the study of their antimicrobial and antioxidant activity *Mater. Lett.* **180** 264–7
- [46] Dipankar C and Murugan S 2012 The green synthesis, characterization and evaluation of the biological activities of silver nanoparticles synthesized from *Iresine herbstii* leaf aqueous extracts *Colloids Surf. B* **98** 112–9
- [47] Siripireddy B and Mandal B K 2017 Facile green synthesis of zinc oxide nanoparticles by *Eucalyptus globulus* and their photocatalytic and antioxidant activity *Adv. Powder Technol.* **28** 785–97
- [48] Jalalvand A R *et al* 2019 Chemical characterization and antioxidant, cytotoxic, antibacterial, and antifungal properties of ethanolic extract of *Allium Saralicum* RM Fritsch leaves rich in linolenic acid, methyl ester *J. Photochem. Photobiol. B* **192** 103–12
- [49] Queiroz Y S *et al* 2009 Garlic (*Allium sativum* L.) and ready-to-eat garlic products: *in vitro* antioxidant activity *Food Chem.* **115** 371–4
- [50] Goorani S *et al* 2019 Assessment of antioxidant and cutaneous wound healing effects of *Falcaria vulgaris* aqueous extract in Wistar male rats *Comparative Clinical Pathology* **28** 435–45
- [51] Kara E *et al* 2010 Effect of zinc supplementation on antioxidant activity in young wrestlers *Biol. Trace Elem. Res.* **134** 55–63
- [52] Chao W-W *et al* 2019 Antioxidant activity of graptopetalum paraguayense E. Walther leaf extract counteracts oxidative stress induced by ethanol and carbon tetrachloride Co-induced hepatotoxicity in rats *Antioxidants* **8** 251
- [53] Moldovan B *et al* 2016 A green approach to phytomediated synthesis of silver nanoparticles using *Sambucus nigra* L. fruits extract and their antioxidant activity *J. Mol. Liq.* **221** 271–8
- [54] Ghavipour M *et al* 2017 Pomegranate extract alleviates disease activity and some blood biomarkers of inflammation and oxidative stress in Rheumatoid Arthritis patients *Eur. J. Clin. Nutr.* **71** 92–6
- [55] Varga M *et al* 2018 Phenolic composition and antioxidant activity of colored oats *Food Chem.* **268** 153–61
- [56] Baschieri A *et al* 2017 Explaining the antioxidant activity of some common non-phenolic components of essential oils *Food Chem.* **232** 656–63
- [57] Amanpour A, Kelebek H and Selli S 2019 LC-DAD-ESI-MS/MS-based phenolic profiling and antioxidant activity in Turkish cv. Nizip Yagli olive oils from different maturity olives. *J. Mass Spectrom.* **54** 227–38

- [58] Parveen M *et al* 2016 Microwave-assisted green synthesis of silver nanoparticles from *Fraxinus excelsior* leaf extract and its antioxidant assay *Applied Nanoscience* **6** 267–76
- [59] Liu D *et al* 2016 Interactions between a phenolic antioxidant, moisture, peroxide and crosslinking by-products with metal oxide nanoparticles in branched polyethylene *Polym. Degrad. Stab.* **125** 21–32
- [60] Hamelian M *et al* 2018 Green synthesis of silver nanoparticles using *Thymus kotschyanus* extract and evaluation of their antioxidant, antibacterial and cytotoxic effects *Appl. Organomet. Chem.* **32** e4458
- [61] Toce M S *et al* 2018 A case report of methadone-associated hypoglycemia in an 11-month-old male *Clinical Toxicology* **56** 74–6
- [62] Kharasch E D *et al* 2008 Mechanism of ritonavir changes in methadone pharmacokinetics and pharmacodynamics: I. Evidence against CYP3A mediation of methadone clearance *Clinical Pharmacology & Therapeutics* **84** 497–505
- [63] Nielsen D A *et al* 2009 Increased OPRM1 DNA methylation in lymphocytes of methadone-maintained former heroin addicts *Neuropsychopharmacology* **34** 867–73
- [64] Li W *et al* 2016 Methadone-induced damage to white matter integrity in methadone maintenance patients: a longitudinal self-control DTI study *Sci. Rep.* **6** 1–8
- [65] He L *et al* 2009 Methadone antinociception is dependent on peripheral opioid receptors *The Journal of Pain* **10** 369–79
- [66] Hsu W Y, Chiu N Y and Liao Y C 2009 Rhabdomyolysis and brain ischemic stroke in a heroin-dependent male under methadone maintenance therapy. *Acta Psychiatrica Scandinavica* **120** 76–9
- [67] Lin W-C *et al* 2012 White matter abnormalities correlating with memory and depression in heroin users under methadone maintenance treatment *PLoS One* **7** e33809
- [68] Wollman S C *et al* 2017 Gray matter abnormalities in opioid-dependent patients: a neuroimaging meta-analysis *The American Journal of Drug and Alcohol Abuse* **43** 505–17
- [69] Costa L G, Pellacani C and Guizzetti M 2017 *In vitro* and alternative approaches to developmental neurotoxicity, in reproductive and developmental *Toxicology*. Second Edition (Germany: Elsevier) pp 241–53
- [70] Tian X *et al* 2017 Neurotoxicity induced by methamphetamine-heroin combination in PC12 cells *Neurosci. Lett.* **647** 1–7
- [71] Badisa R B *et al* 2018 Identification of biochemical and cytotoxic markers in cocaine treated PC12 cells *Sci. Rep.* **8** 1–14